THE INFLUENCE OF VARIABILITY OF RAINFALL AND SOIL MOISTURE ON EVAPORATION FROM SEMI-ARID AREAS

G. Dugdale
University of Reading.
Reading, U.K.

1. INTRODUCTION

The proper representation of evaporative fluxes from the surface to the atmosphere is an important feature of many general circulation models.

In areas where the potential evapotranspiration significantly exceeds the rainfall the actual evaporation is limited by the soil moisture. This situation pertains over wide regions of the semi-arid and seasonally arid tropics and sub tropics. Here, because the energy inputs at the surface from radiation and the atmosphere are relatively constant from day to day, the soil moisture is the dominant control on evaporation. Hence, in these regions the soil moisture and its spatial distribution needs to be defined. The direct, daily measurement of soil moisture and its variability in space is at present not possible so it must be modelled. This is usually achieved by maintaining a surface water budget in which the rainfall is the source and evaporation and run- off are the sinks. The average rainfall over a model grid may be derived from model forecasts or from observations. In either case a knowledge of the variation of the rainfall within the grid and its subsequent redistribution by surface and sub-surface run-off is needed. Only then can the soil moisture and hence evaporation be modelled.

This paper describes the results of a series of experiments designed to establish the variability of daily rainfall over the Sahelian zone on scales up to 4×10^4 km^2 and experiments to investigate the local run-off in areas without external drainage. A simple bare soil evaporation model is used to illustrate the importance of the spatial inhomogeneity of the soil moisture to area evaporation.

2. THE STUDY REGION

The surface and satellite data used in this study have been derived mainly from the Republic of Niger with extensions east and west across the Sahelian zone. The Sahel and the adjoining areas have been variously described (for example Nicholson (1981)). For the purposes of this paper we are concerned with the seasonally arid area to the south of the Sahara extending from about 12°N to 19°N and 15°W to 32°E. Except for the Mara mountains at about 24°E the terrain is without major relief. The annual rainfall ranges from about 800mm in the south to 100mm in the north. The wet season starts in May and ends in September in the south, but may only last for a few weeks in the north.

Almost all rainfall is convective in origin and, while local storms are common, most the rain comes from large cloud clusters. In the western half of the region these clusters are usually in the form of line squalls which may have lifetimes of several days. In the east the storms have a stronger diurnal signal tending to decay during the early morning hours. These cloud clusters are typically of 200 to 400km in diameter and can be identified in the thermal infra-red imagery of the satellite data by their low cloud top temperatures.

3. SPATIAL VARIABILITY OF DAILY RAINFALL

Rainfall estimates derived from G.C.M's or raingauge data give inadequate information on the distribution of the rainfall within a grid element. In areas where convective storms are the main source of rainfall the whole of a grid element may not be affected by a storm and raingauge networks are too sparse to estimate the rain- free fraction. Over those areas that are wetted the rainfall will usually be uneven. The yield at any site is mainly determined by the vigor and proximity of the nearest storm cells. Only calibrated radar can provide data on these two factors and this is not available in the areas of interest. An alternative is to use satellite data to determine the larger scale rainfall pattern (Dugdale (1986)) and combine this with the characteristics of small scale spatial variations of rainfall from storms typical of the study area.

3.1 Small scale variability of rainfall.

On scales of up to 20km the rainfall from individual storms can be monitored only by radar or by a very dense raingauge network. Earlier work on point and area rainfall had been carried out using dense networks of raingauges (e.g. Osborne et al. (1979)) or radar (e.g. Barnston & Thomas (1983)). These studies referred to the United States of America and no detailed data was available for the Sahel. Accordingly, in the absence of radar an experiment was carried out in 1985 and 1986 using raingauges at Ibecetene (15.3°N, 5.9°E) in the Republic of Niger. (Flitcroft et al (1988)).

The network which consisted of 36 raingauges in a square grid at 2km spacing was operated in the 1985 and 1986 wet seasons. The rainfall at each gauge was measured after each event. Of the 35 recorded events 25 covered the whole grid. The remaining 10 more localised storms only contributed 4% to the total rainfall. In the analyses only the data from the widespread events was used.

When sampled at 2km the rainfalls were usually coherent as can be seen from figure 3.1 which shows the yields from two typical events. Figure 3.2 shows the reduction in correlation of rainfall events as the separation increases. This correlation diagram is typical of others derived elsewhere in the Sahel.

The data was used to relate the point to area average rainfall. The latter being taken as the average of the point rainfalls in the grid.

Figure 3.3 shows the interquartile ranges of the rainfall, plotted as a function of the area mean rainfall. It is seen that there is a lot of scatter but that, except for the two heaviest rainfalls, the I.Q.R. is approximated by half of the area mean rainfall.

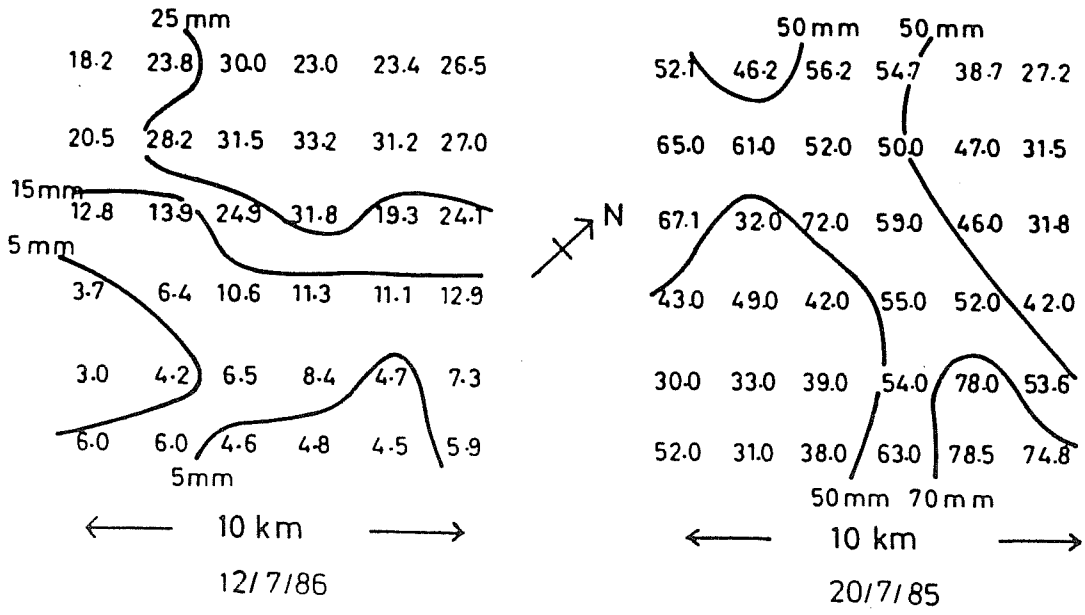

Figure 3.1
Raingauge measurements from typical storms over Ibecetene.

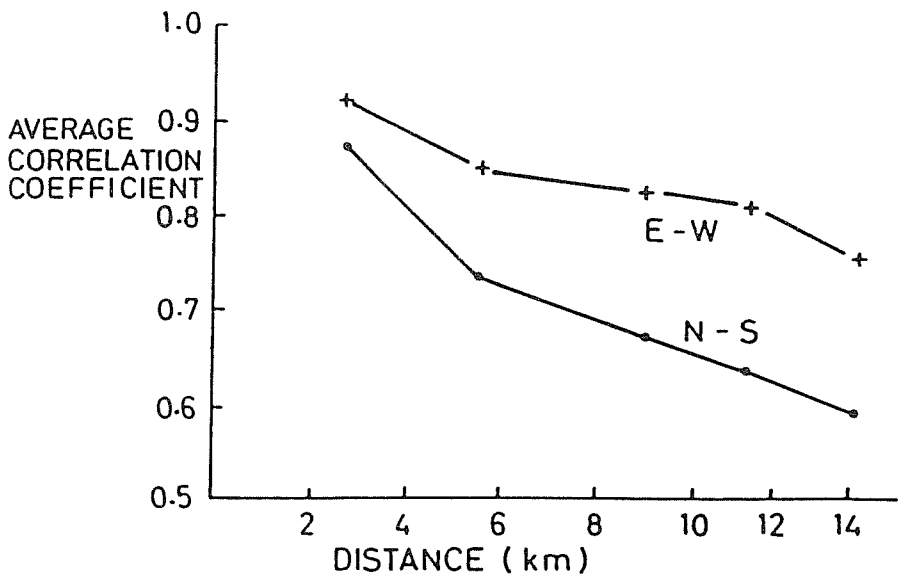

Figure 3.2
Correlation coefficients of rainfall amounts measured at Ibecetene as a function of raingauge separation.

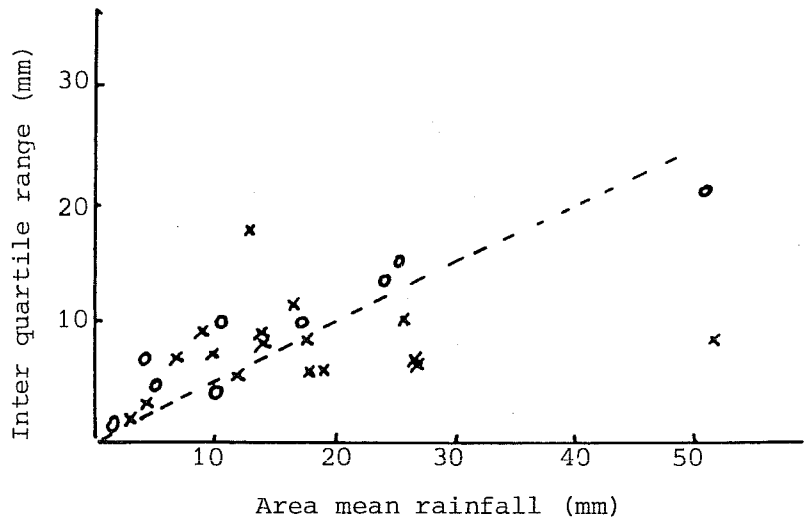

Figure 3.3 The inter quartile range of point rainfall associated with the area mean rainfall over a 10km square. o 1985: x 1986.

3.2 Variability of rainfall on scales up to 200km

The variation of rainfall from individual storms on scales up to 200km can only be determined by an observational system which either gives a virtually continuous spatial coverage or which represents all scales above 15km or so which can then be combined with statistical data on the smaller scale variability. Satellite data can give an indication of the rainfall from convective clouds on scales from 5 or 10km upwards. Since the mid 1970's many studies have been made into the use of thermal infra-red data from geostationary satellites to monitor rainfall. A comparison (Snijders (1988)) of different techniques applied in the Sahel showed that cold cloud duration has some skill as an estimator of rainfall but that the discrimination between rainfall amounts was not good. The method used by the University of Reading group gave a standard deviation between raingauge measured and satellite estimated rainfall of 1.1 classes where the classes are defined as in table 3.1.

Class	1	2	3	4	5	6	7
Daily rainfall (mm)	1	1-5	6-10	11-20	21-40	41-80	80

Table 3.1 Classes of rainfall used by Snijders 1988 in assessing satellite estimates of rainfall.

Flitcroft (1988) shows that the standard sampling error caused by using point measurements to validate area estimates of rainfall derived from satellite data is 6mm. Sniders' and Flitcroft's results cannot be directly linked; however, the 6mm uncertainty corresponds to almost one class over the most common range of rainfalls. It therefore appears that much of the difference noted by Snijders arises from the sampling error. Further, recent results by Hardy et al (1988) show that daily rainfall estimates averaged over areas of order $10^4 km^2$ give useful estimates of the daily rainfall.

The above findings lead us to believe that the variations of daily cold cloud duration over areas of this size may indicate the rainfall variability. They will, however, somewhat underestimate it as it is well known that satellite rainfall estimates fail to identify the heaviest local storms. (Barrett (1986)).

Figure 3.4, reproduced from Dugdale (1986), shows the fraction of a 200 x 200km square covered by cold ($< -60°C$) cloud as a function of the daily CCD over the square. This was constructed using 21 thermal infra-red Meteosat images per day for July 1985. The area covered is shown in figure 3.5 which included 60 200 x 200km squares. The typical rainrate associated with cold cloud of -60°C in these latitudes and seasons is 4.5mm/hr. Hence grid area mean rainfalls of 10mm would have mean CCD of about 2 hours and some 20% of the grid would be rain free.

Figure 3.4

Mean fraction of a 200 x 200km square with zero CCD against mean CCD for that grid square.

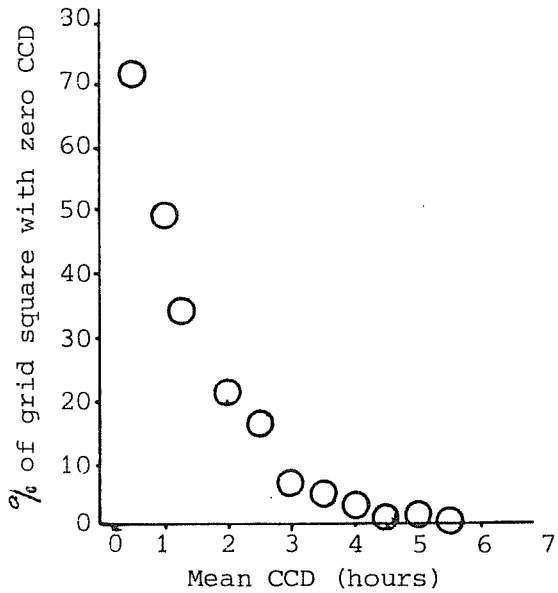

Figure 3.5
Showing the areas covered by the satellite data used in the studies in 1985 and 1987 and the zone surrounding Ibecetene (shaded).

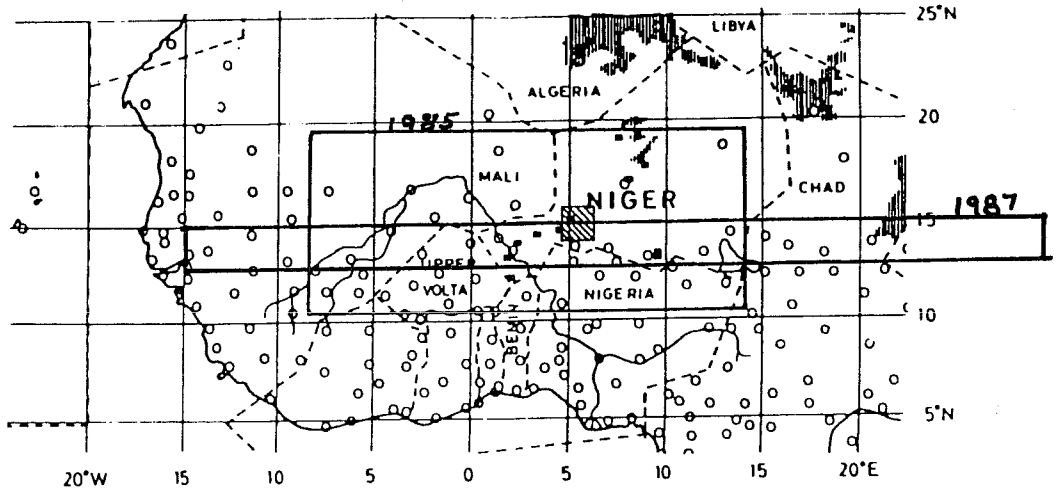

Further studies on 1987 Meteosat data for a similar latitude belt of the Sahel have identified not only the cloud free fraction of grid squares of 100km side length but the spatial variation of the CCD within the cloud affected area. A temperature threshold of -50°C has been used which, for the zone in question (13°N to 15°N), correctly identified 95% of the rain/no rain ten-day periods and divided the erroneous classifications almost equally between rainy/cloud-free and dry/cloudy contingencies. The mean rain per hour of cold cloud was 2.9mm. Twenty-four thermal infra-red images per day were used in this study which includes 188 grid elements each 20 x 20 Meteosat pixels (about 100 x 100km). Analysis of daily data throughout July yields 2728 samples.

Figure 3.6. shows the fraction of grid squares with zero cold cloud as a function of the grid area average cold cloud duration. A sub-scale on the diagram indicates the rainfall associated with the cold cloud using the above relationship. The cloud-free fraction of a grid associated with grid average cold cloud is less than that in the Dugdale (1986) study. This arises partly from the use of a different (warmer) cold cloud threshold and partly from the change in grid size.

Figure 3.6
The fraction of cloud-free pixels associated with different grid area (100 x 100km) average daily cold cloud durations. July 1987, Sahel 13-15°N.

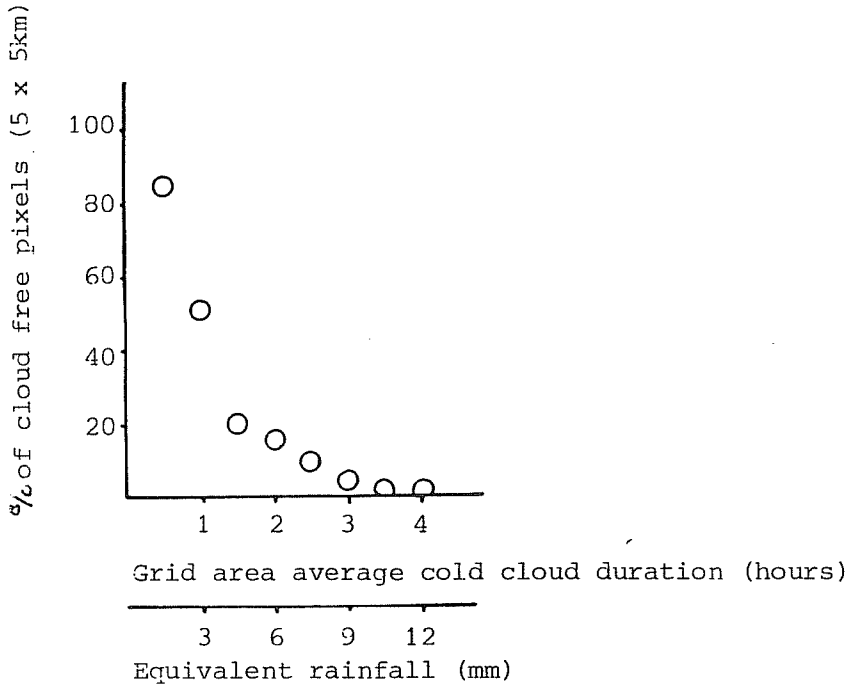

The frequency distributions of cold cloud duration within the grid have been calculated for each grid-area-average cold cloud duration. These are listed in table 3.2. Three, corresponding to grid-area-average durations of 1, 2.5 and 5 hours are illustrated in figure 3.7. Longer durations than 5 hours present similar curves to that for 5 hours but translated along the x axis.

Figure 3.7
Percentage distribution of cold pixels (5 x 5km) associated with three different grid (100 x 100km) area average cold cloud durations. July 1987, Sahel 13-15°N.

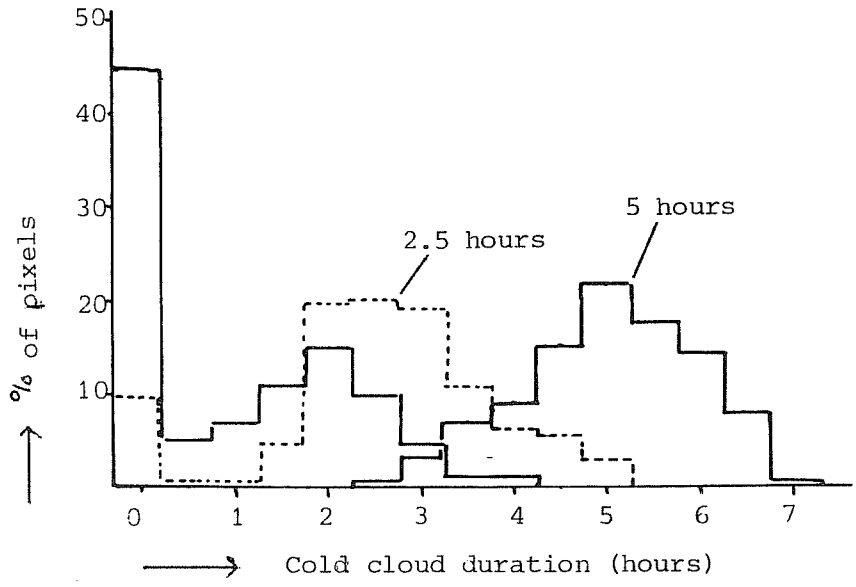

Table 3.2

Percentage of a 100 x 100km grid square influenced by cold cloud (< -50°C) cloud as a function of the grid-area-average cold cloud duration. 13°N to 15°N over the Sahel, July 1987.

Cold cloud duration (hours)	Grid area average cold cloud duration (hours)								
	1.0	1.5	2.0	2.5	3.0	3.5	4.0	4.5	5.0
0	45	20	17	9	4	2	2	1	0
0.5	5	6	2	1	1	0	0	0	0
1.0	7	13	5	1	4	0	0	0	0
1.5	12	22	10	4	7	1	1	1	0
2.0	15	18	20	20	9	5	1	1	0
2.5	9	12	16	20	12	6	5	3	1
3.0	4	8	14	18	20	10	7	6	3
3.5	1	2	10	11	18	27	12	11	7
4.0	1	1	5	7	1	27	26	18	11
4.5			1	6	8	14	20	21	15
5.0				3	6	7	17	13	22
5.5						2	7	9	18
6.0						1	2	7	14
6.5								6	8
7.0								3	1

3.3 Total variability

Combining the results described in sections 3.1 and 3.2 would give the total variability of the rainfall in a grid square. To achieve this we must use the results in section 3.1 to model the small scale variability and attribute a rainfall per hour of cold cloud to the relationships described in section 3.2. Comparison of the cold cloud (< -50°C) in this region with raingauge measurements gives a mean rainfall of 2.9mm per hour of cold cloud duration. Within an actual event over half this rain will actually occur in the first 30 minutes of the storm. (Milford & Dugdale (1984)).

The sample of data from the small scale experiment (section 3.1) is inadequate to properly model the rainfall distribution over the rainfall range. However, as we are interested in estimating the influence of the spatial variability on the evaporation we can perhaps use a fairly crude model. For the average falls (8 - 16mm) the rain is distributed approximately normally about the mean value with a standard deviation of 0.35 of the mean value. For this argument we have adapted this model throughout the range of rainfalls studied, sub-zero values being set to zero. There is insufficient data at low rainfalls to establish the parameters for the more popularly used gamma distribution of rainfall amounts.

Imposing the small scale variability on the large scale distribution produces the curves shown in figures 3.8 a,b and c. As expected the distribution curves are broader; the frequency of the most popular non-zero class being approximately halved. The influence of this distribution on subsequent evaporation is discussed in section 5.

Figure 3.8
The percentage of pixels (solid line) and the percentage of area (pecked line) associated with different rainfall amounts for grid area average rainfalls of (a) 3mm, (b) 7.5mm and (c) 15mm.

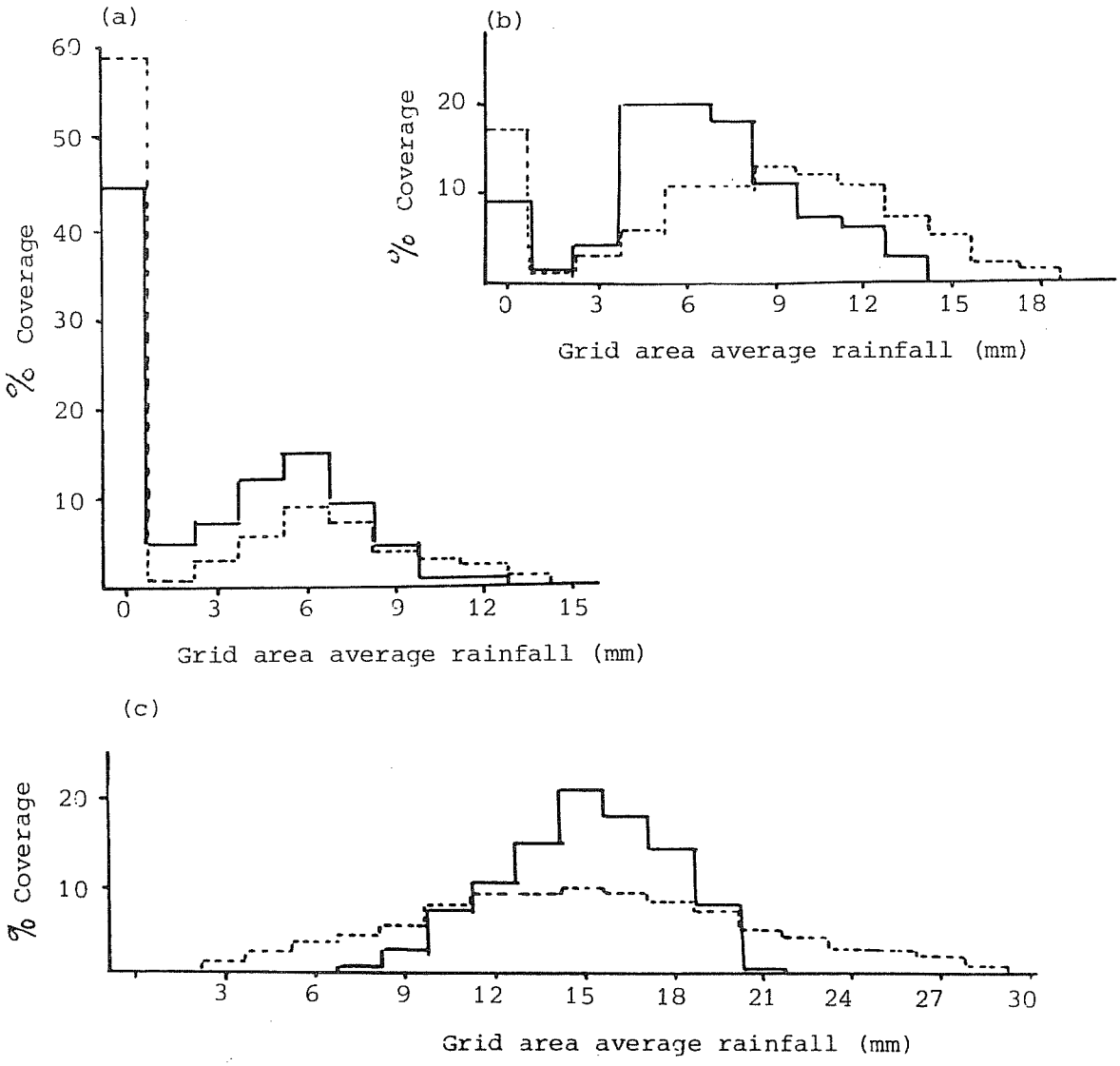

4. EFFECTS OF SURFACE RUN-OFF

Many parts of the semi-arid tropics are not drained to the oceans, and even in those that are the run-off from the area is usually an insignificant fraction of the water budget of that area. However, local run-off within the area is important in that it redistributes the rainfall, hence alters the evaporation patterns (and allows vegetation to grow preferentially in favoured areas). This local run-off may be of a scale of only a kilometre or so. It is a function of the terrain, soil type, vegetative cover and rainfall rates.

In 1985 and 1986 experiments were made to investigate the influence of run-off in lightly undulating Sahelian terrain. The scale length of the undulations is about 1km and the amplitude 10km. Gravimetric sampling of soil moisture in the upper layers was complimented by use of the neutron scattering technique to depths of 1.6m. Two sites, one at the top of an incline, the other a few hundred metres away, near the base, were monitored daily. At each site the soil was maintained in different conditions on two sub-sites; one bare, the other naturally vegetated.

Figure 4.1 shows the influence of vegetation on the soil moisture in the upper 1.6m of the soil near a dune crest. Each curve represents the average of two sets of readings from similar plots. Early in the season the differences are due to minor local topographic and soil characteristics of the sites. It is seen that as the season develops and grass grows so a 60mm difference in the stored water develops and the evaporative loss from the vegetated area exceeds that from the bare soil by about 1.5mm per day. Immediately after rainfall neither plot retains all the precipitation, implying a contribution to run-off. Figure 4.2 shows the corresponding curves at the lower site. In the roughened, bare plots soil moisture increases by several times the rainfall after major rainfall events, indicating significant run-on. However, on the adjacent vegetated plots the soil moisture only rose by about the same amount as the rainfall. This implies that water was running horizontally through the vegetated plots to accumulate lower in the drainage system. Rainfall events of less than 8mm did not appear to cause run-on to the lower, roughened, bare plot.

These experiments do not allow us to estimate the run-off over extended areas; nor would such information be useful unless we know the relative areas of the "source" and "sink" zones. These areas are themselves a function of the topography, soil type, soil moisture, vegetation and rainfall rate. The lightest falls give rise to little run-off; average rainfalls (18 to 16mm) will give run-off to adjacent depressions or, if these are saturated, to the major more distant depressions which will also always benefit from the most intense storms.

Figure 4.1
Time series of soil moisture and rainfall at an elevated level site. Ibecetene, 1986.

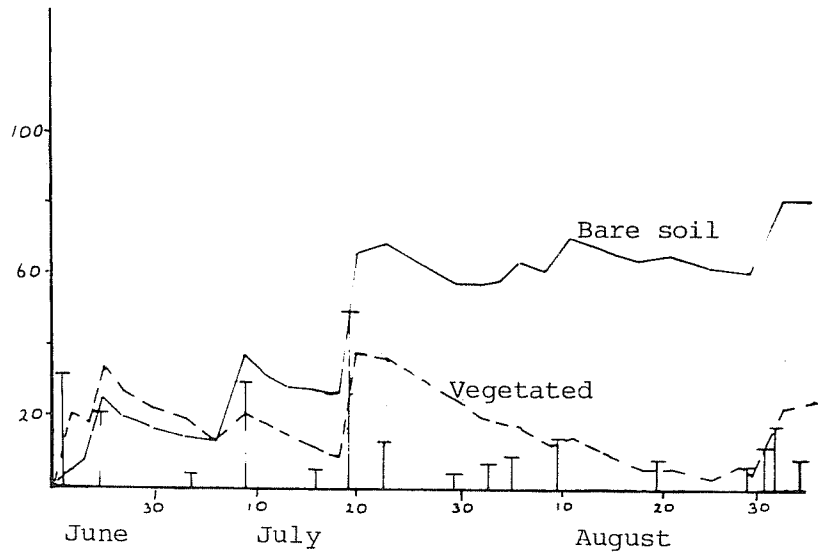

Figure 4.2
Time series of soil moisture at a level site in a depression. Ibecetene, 1986.

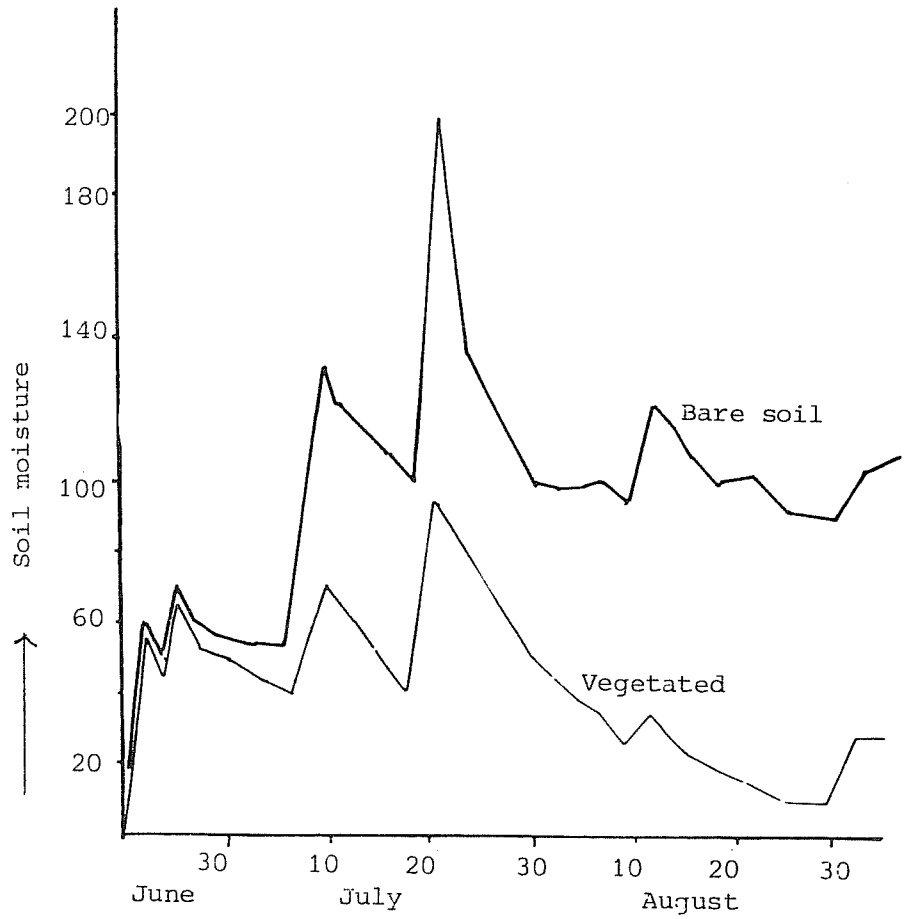

5. EVAPORATION ESTIMATES

Evaporation in the semi-arid and seasonally arid tropic usually takes place from mainly bare soil at the start of the rainy season, from sparse scattered vegetation in the growing season and from isolated wadis or seasonal oases after the end of the rains.

Evaporation from the bare soil is controlled largely by the rainfall and evaporation during the previous week or so. The vegetation transpires according to the atmospheric demand and the physiological state of the plants which includes their access to soil moisture. Evaporation from seasonal ponds and their surrounding vegetation is strongly influenced by the advection of air over the drier surroundings. Non of the existing operational evaporation models attempts to represent these conditions. It is probable that the bare soil and vegetated areas will have to be treated separately, the fraction of a grid attributed to each surface type being derived from other data sources. These could be from a geographical, seasonally varying, data base or from satellite observations.

Inhomogeneities in grid area rainfall affect evaporation in two main ways: evaporation is reduced in places with below average rainfall and run-off is enhanced from those areas receiving increased rainfall. This run-off is concentrated in small areas from where it may be evaporated over a long period giving rise to a low grid-area average background evaporation which may continue well into the dry season.

The reduction in short term evaporation from bare soils due to the inhomogeneous rainfall may be investigated by applying a simple bare soil evaporation model to the rainfall distributions illustrated in section 3.3.

Data from the experiment described in section 4 and from many years soil moisture and rainfall records over the Sahel show that the daily evaporation (E) may be well represented by

$$E = PE \times d^{-1} \times 0.7\text{mm}$$

where d is the number of days since rainfall and PE is the mean potential evapotranspiration derived from climatological data. The classical form of this simple equation gives $d^{-0.5}$ from the diffusion theory. However, our data shows a better fit for d^{-1}. This may be due partly to the strong thermal gradients in the soil subduing evaporation in the daytime.

In order to study the evaporation from bare soil in the two weeks following rainfall the above evaporation formulae, with PE at 130mm/month, has been applied to three representations of grid area rainfall. First assuming the rain is evenly distributed, second assuming the rain is evenly distributed over the wetted area, and thirdly that the rainfall was distributed according to section 3.3. The results are illustrated in figure 5.1(a),(b) and (c), representing rainfalls of 3, 7.5 and 15mm respectively.

For the light rainfall case the grid area average model returns all the rain to the atmosphere on the first day following rainfall. Assuming the rain to be evenly spread over the wetted area results in 0.4 of the rainfall being evaporated on the first day and the rest within seven days. The fully distributed rainfall model spreads the evaporation over two weeks. Given a typical rain event spacing of five to ten days the effects of non uniform rainfall are not only to delay evaporation but to conserve some moisture for future transpiration by crops.

Evaporation after rainfalls of 7.5mm are strongly influenced by the distribution of rainfall within a grid square (figure 5.1(b)). A difference of 0.35mm on the first day increasing to an accumulated difference of 1mm by day five and 2mm after two weeks. The evaporation immediately after rainfall events of 15mm or more are less influenced by the expected variation of the rainfall within a grid square (figure 5.1(c)): the change from even to unevenly distributed rainfall resulting in a difference in evaporation of about 1mm accumulated over two weeks.

This analysis raises the question of how much of the rainfall comes from rain events after which the evaporation is significantly influenced by the distribution of the rainfall. The analysis of the satellite data allows us to answer this by assuming that our clouds on average identify rain areas and attributing 2.9mm of rainfall to each hour's duration of cold ($< -50°C$) cloud. This is shown in figure 5.2 below, from which it is seen that half the rainfall is derived from events giving grid area average rainfall of about 10mm.

While we do not attempt to quantify the area run off, or specify where run-off accumulates, it is clear that the non-uniform grid area rainfall will significantly enhance run-off. Over the soils and terrain used for our field experiment it appears that little run-off occurs from falls of less than about 7mm. Above this amount the run-off/rainfall relationship is strongly non-linear (Shuttleworth (1988)). It is seen from figures 3.8 that even the 3mm grid area average rainfall gives some rain in excess of 7.5mm while the 10mm grid area average may be expected to give falls of 18mm locally.

Figure 5.1
Grid area (100 x 100km) average evaporation from bare soil as a function of time since rainfall using different models of rain distribution
(i) even distribution over the grid,
(ii) Even distribution over the wetted area
(iii) Modelled distribution (see section 3.3)
for grid average rainfall of 3mm (a), 7.5mm (b) and 15mm (c).

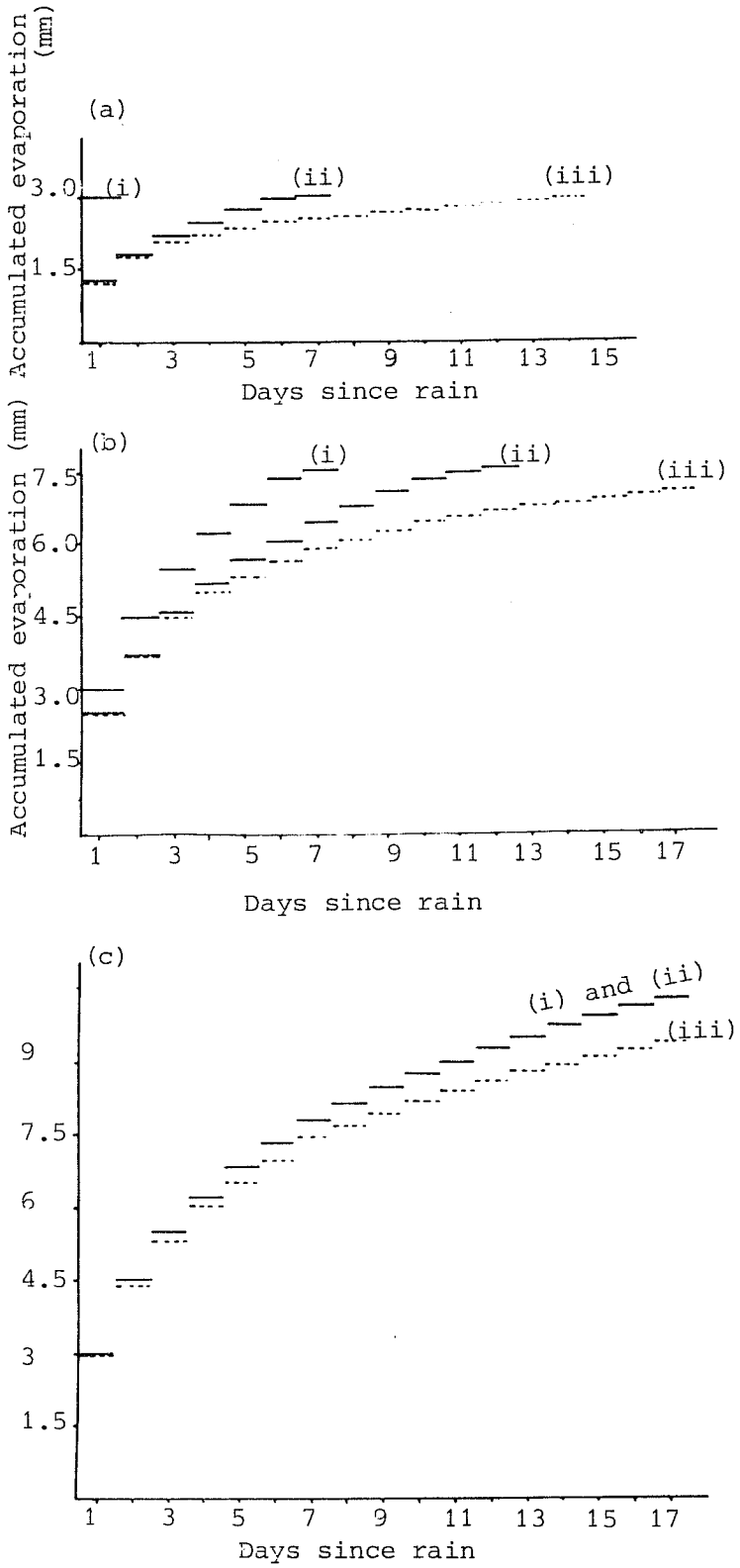

Figure 5.2
Percentage contribution of daily rainfall events of different area grid averages to the monthly total. July, 1987, Sahel 13-15°N.

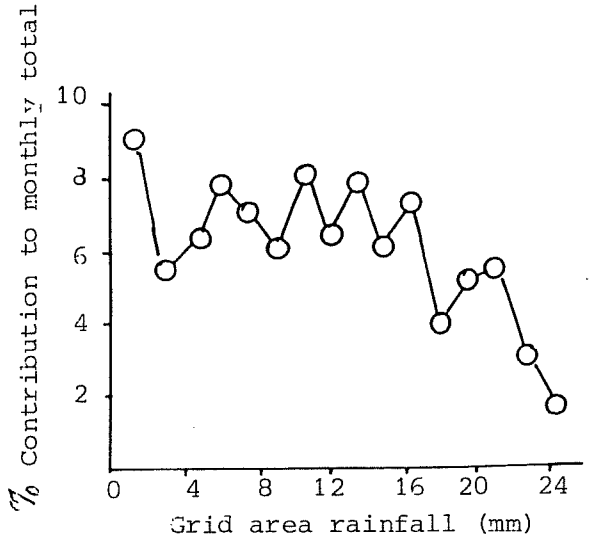

6. DISCUSSION

The purpose of this paper was to illustrate the influence of spatial variability of rainfall on evaporation, with particular reference to semi-arid areas where much of the evaporation is from bare soil. Though the models used may be somewhat simplistic it is clear that this distribution problem must be considered in GCMs where the evaporative input is an important feature of the model. The influence of non-uniform rainfall is to decrease the initial evaporation by reducing the well wetted area and to extend the evaporative period from areas favoured by high rainfall or run-off. The last feature allows a low rates of evaporation to continue long into the dry season from seasonal ponds.

It appears that in zones of low vegetative cover and high potential evaporation the actual evaporation from bare and vegetated areas may have to be treated separately. Apportionment of the areas could be derived from satellite derived vegetation indices or geographical data bases - if such exist with the necessary seasonal detail.

While drawing attention to a particular problem this paper offers little help with solutions. However, studies over a range of semi arid Africa show that the small scale spatial distribution of rainfall measured over the Sahel is fairly typical. Further analyses of satellite data should investigate how far the larger scale variability can be generalised. This would allow the development of mean rainfall distribution dependant on the grid area average rainfall and geographic area.

One may envisage the eventual incorporation of real time satellite cloud data to give the actual distribution of convective rainfall within GCM grid elements rather than imposing mean distribution properties.

7. ACKNOWLEDGEMENTS

The various experimental results quoted in this report have come from the combined work of the TAMSAT group at the University of Reading; the principal researchers being J.R. Milford, I.D. Flitcroft, M. Saunby & V. McDougall. The research has been funded by the Overseas Development Administration of the United Kingdom, the United Nations Food & Agriculture Organisation and the European Commission.

REFERENCES

Barrett,E.C., D'Souza,G. & Power,C.H., 1986: Comparison of two Meteosat rainfall monitoring techniques applied to part of the western Sahel. Proc. 6th Meteosat Scientific Users Meeting, Amsterdam 1986, EUMETSAT.

Barnston,A.G. & Thomas,J.L., 1983: Rainfall measurement accuracy in FACE: A comparison of gauge and radar rainfalls. J.of Climate & Applied Met., 23, 2038-2052.

Dugdale,G., Milford,J.R. & Rowell,D.P., 1986: Using Meteosat data to relate rainstorms over the West African Sahel to data on the scale of the ECMWF grid. Proc. of 6th Scientific Users Meeting, Amsterdam. EUMETSAT.

Flitcroft,I.D., Milford,J.R. & Dugdale,G., 1988: Relating point to area average rainfallin semi-arid West Africa and the implications for rainfall estimates derived from satellite data. Accepted for publication in J.of App. Met.

Milford,J.R. & Dugdale,G, 1984: Short period forecasts in West Africa using Meteosat data. Proc. Nowcasting-II Symposium, Sweden, Sept 1984 (ESA SP-208)

Nicholson,S.E., 1981: Rainfall and spheric circulation during drought periods and wetter years in West Africa. Mon.Wea.Rev., 109, 2191-2208.

Osborne,H.B., Renard,K.G. & Simanton,J.R., 1979: Dense networks to measure convective rainfall over the South Western United States. Water Resources Research, 15, 1701-1711.

Shuttleworth,W.J., 1988: Macrohydrology - the new challenge for process hydrology. J.of Hydrology, 10, 31-56.

Snijders,F.L., 1988: An evaluation of techniques for monitoring of rainfall over the western Sahel using Meteosat PDUS data. Proc. of the 7th Meteosat Scientific Users Meeting, Madrid 1988. EUMETSAT.